Published in final edited form as:
Nutr Metab Cardiovasc Dis. 2014 April ; 24(4): 384–392. doi:10.1016/j.numecd.2013.09.006.

Increased density of inhibitory noradrenergic parenchymal nerve fibers in hypertrophic islets of Langerhans of obese mice

I. Giannulis[a,1], **E. Mondini**[a,1], **F. Cinti**[a], **A. Frontini**[a], **I. Murano**[a], **R. Barazzoni**[b], **G. Barbatelli**[a], **D. Accili**[c,**], and **S. Cinti**[a,*]

[a]Dpt of Experimental and Clinical Medicine, Obesity Center, University of Ancona (Politecnica delle Marche) and Azienda Ospedali Riuniti, 60020 Ancona, Italy

[b]Dpt of Medical, Surgical and Health Sciences, Clinical Medicine, University of Trieste, Trieste, Italy

[c]Naomi Berrie Diabetes Center, Dpt of Medicine, College of Physicians & Surgeons of Columbia University, New York, NY 10032, USA

Abstract

Background and aim—We sought to identify mechanisms of beta cell failure in genetically obese mice. Little is known about the role of pancreatic innervation in the progression of beta cell failure. In this work we studied adrenergic innervation, in view of its potent inhibitory effect on insulin secretion. We analyzed genetically obese *ob*/*ob* and *db*/*db* mice at different ages (6- and 15-week-old), corresponding to different compensatory stages in the course of beta cell dysfunction. 15 week-old HFD mice were also studied.

Methods and results—All mice were characterized by measures of plasma glucose, insulin, and HOMA. After perfusion, pancreata were dissected and studied by light microscopy, electron microscopy, and morphometry. Insulin, Tyrosine Hydroxylase-positive fibers and cells and Neuropeptide Y-positive cells were scored by immunohistochemistry.

Islets of obese mice showed increased noradrenergic fiber innervation, with significant increases of synaptoid structures contacting beta cells compared to controls. Noradrenergic innervation of the endocrine area in obese *db*/*db* mice tended to increase with age, as diabetes progressed. In *ob*/*ob* mice, we also detected an age-dependent trend toward increased noradrenergic innervation that, unlike in *db*/*db* mice, was unrelated to glucose levels. We also observed a progressive increase in Neuropeptide Y-immunoreactive elements localized to the islet core.

Conclusions—Our data show increased numbers of sympathetic nerve fibers with a potential to convey inhibitory signals on insulin secretion in pancreatic islets of genetically obese animals, regardless of their diabetic state. The findings suggest an alternative interpretation of the pathogenesis of beta cell failure, as well as novel strategies to reverse abnormalities in insulin secretion.

[*]Corresponding author. Tel.: +39 071 2206088; fax: +39 071 2206087. s.cinti@univpm.it, cinti@univpm.it (S. Cinti). [**]Corresponding author. Tel.: +1 212 851 5332; fax: +1 212 851 5335. da230@columbia.edu (D. Accili).
[1]These authors contributed equally to this work.

Keywords

Islets; Noradrenergic fibers; Obesity

Introduction

Type 2 diabetes is associated with progressive loss of pancreatic beta cell function and mass [1]. Recent data suggest a pivotal role for chronic low-grade inflammation of visceral adipose tissue in the pathogenesis of metabolic disorders associated with obesity [2–7]. The mechanism by which tissue inflammation impinges on insulin sensitivity is unclear, but possibly involves direct impairment of insulin action and insulin signaling through its biochemical pathways [8–10]. The gradual transition of insulin resistance into type 2 diabetes is usually linked with a change in pancreatic islet composition. During compensated insulin resistance, pancreatic islets are conspicuous by their hypertrophy, resulting from increased cell number and size [11,12]. But as compensation fails, islet mass gradually decreases, and beta cells become depleted of their characteristic insulin secretory granules [11,13]. These observations suggest that factors produced or acting during the progression of insulin resistance affect beta cell compensation. Much effort has been devoted to identifying potential beta cell growth factors as well as factors that affect beta cell injury, for example through cytokine release or generation of reactive oxygen species and oxidative stress. Evidence for such mechanism is abundant, if circumstantial [14].

Recently, it has been demonstrated that sympathetic innervation of the islet increases in experimental diabetic mice [15], and that insulin secretion is dependent on the autonomic nervous system tone [16]. Considerably less is known about the role of pancreatic innervation in the progression of beta cell failure in obesity [17–19]. To address this question, we studied the innervation of the islets of Langerhans in two strains of genetically obese mice (*ob*/*ob* and *db*/*db*) at two different stages in the development of their obesity and diabetes, corresponding to different compensatory stages in the natural history of beta cell dysfunction. We focused on adrenergic innervation in light of the fact that little is known about it, despite the potent inhibitory effect of noradrenergic stimulation on insulin secretion [17–21].

Methods

Animals

All animal procedures were in accordance with the principles of laboratory animal care. Fifty female mice were purchased from Harlan (Udine, Italy) and subdivided in two groups. The first group was comprised of twenty 6-week-old animals: five obese B6.V-Lep^{ob}/OlaHsd, (hereafter, *ob*/*ob*) and five lean control mice (hereafter, *ob*/+); five diabetic BKS.Cg^{-}+Lepr^{db}/+Lepr^{db}/OlaHsd (hereafter, *db*/*db*) and five lean control mice (hereafter, *db*/+). The second group included thirty 15-week-old animals: five obese B6.V-Lep^{ob}/OlaHsd (hereafter, *ob*/*ob*) and five lean control mice (hereafter, *ob*/+); ten diabetic BKS.Cg^{-}+Lepr^{db}/+Lepr^{db}/OlaHsd (hereafter, *db*/*db*) and ten lean controls (hereafter, *db*/+). Ten female Swiss CD-1 mice aged 3 weeks were weighed and divided into two groups with

similar mean body weight: one group (HFD mice) were fed a high-fat diet (Charles River; 50 kJ% from fat, 30 kJ% from carbohydrates and 20 kJ% from proteins) for 12 weeks; the other group (control mice) were fed with chow diet. Mice were fasted for 4 h and bled for determinations of plasma glucose (mg/dl), insulin (ng/ml) concentration and HOMA prior to euthanasia with Avertin (Fluka Chemie, Buchs, Switzerland). Mice were perfused with 4% paraformaldehyde in 0.1 mol/l phosphate buffer (PB), pH 7.4, for 5 min. Pancreata were dissected using a Zeiss OPI1 surgical microscope (Carl Zeiss, Oberkochen, Germany) and assessed by light microscopy, immunohistochemistry and morphometry.

Light microscopy and morphometry

After dissection, pancreata were further fixed by immersion in 4% paraformaldehyde in 0.1 mol/l sodium Phosphate Buffer, pH 7.4, overnight at 4 °C, then dehydrated, cleared and paraffin embedded. Three sections from different levels (every 0.5 mm) of each tissue were analyzed for exocrine and endocrine area, islets size and density. For each level, 3 μm-thick serial sections were obtained for hematoxylin and eosin staining, and for immunohistochemistry.

Tissue sections were imaged with a Nikon Eclipse E800 light microscope using a 40× objective and digital images were captured with a Nikon DXM 1200 camera. The Nikon LUCIA IMAGE (version 4.61; Laboratory Imaging, Praha, Czech Republic) was used for morphometric analysis. We estimated area of Tyrosine Hydroxylase positive (TH+) fibers as area of TH + fibers/100 μm^2 of endocrine or exocrine area and number of TH+ and Neuropeptide Y positive (NPY+) cells/ 100 μm^2 of endocrine area. The distribution of NPY + cells in islets was also evaluated (number of NPY + cells abutting the periphery of islets and number of NPY + cells scattered in the center of islets/100 μm^2 of endocrine area).

Immunohistochemistry

For immunohistochemistry, 3-μm-thick dewaxed serial sections were incubated with anti-TH (polyclonal rabbit anti-tyrosine hydroxylase, Chemicon-Millipore, Temecula, CA, 1:600), anti-NPY (polyclonal rabbit anti-Neuropeptide Y, Sigma, St. Louis, 1:800) and anti-insulin (polyclonal guinea pig anti-insulin, Abcam, Cambridge, UK, 1:100) primary antibodies according to the Avidin Biotin Complex method. We used 0.3% hydrogen peroxide to inactivate endogenous peroxidase, followed by normal goat serum to reduce nonspecific staining. Consecutive serial sections were incubated overnight (4 °C) with primary antibodies. Biotinylated HRP-conjugated secondary antibodies were goat anti-rabbit IgG and goat anti-guinea pig IgG (Vector Laboratories, Burlingame, CA, USA). Immunohistochemical reactions were performed using Vector's Vectastain ABC Kit (Vector Laboratories, Burlingame, CA, USA) and Sigma Fast 3,3′-diaminobenzidine as substrate (Sigma, St. Louis, MO). Sections were counterstained with hematoxylin.

Confocal microscopy

For immunofluorescence and confocal microscopic analysis, animals were perfused as described above and tissues were post-fixed by overnight immersion. After a brief wash in PB, they were cryoprotected in a solution of 30% sucrose in PB for 24 h at 4 °C. A glass beaker containing 2-methylbutane (isopentane) was cooled in liquid nitrogen, and specimens

were embedded in optimal cutting temperature medium (OCT, Tissue-Tek; Sakura Finetek Europe, The Netherlands), frozen and stored at −80 °C. For the double-labeling experiments, 7-μm-thick cryosections obtained with a CM1900 cryostat (Leica Microsystems; Vienna, Austria) were collected and air-dried overnight at room temperature. After two 15-min washes in PB, sections were incubated in 1:75 normal donkey serum (Jackson Immuno Research; West Grove, PA) in PB for 20 min at room temperature to block nonspecific sites and then incubated overnight at 4 °C with a mixture containing the primary antibodies against insulin and against TH or NPY at 1:100 and 1:600 and 1:800, respectively.

Transmission electron microscopy

Tissue fragments measuring about 1 mm^3 were immersed in a fixative consisting of 2% glutaraldehyde and 2% paraformaldehyde in 0.1 mol/l PB, pH 7.4, for 4 h. They were then washed with PB, postfixed in 1% OsO_4 for 60 min at 4 °C, dehydrated in acetone and embedded in an Epon-Araldite mixture. Thin sections were obtained with an MTX ultra-microtome (RMC, Tucson, AZ, USA), stained with lead citrate, and examined with a Philips CM 10 transmission electron microscope (Philips, Eindhoven, The Netherlands). Synaptic structures were defined as structures filled with vesicles of different electron density, dimensions and shape, and with post-synaptic densities. They were counted and used to calculate the density as number of synaptic structures/ 100 μm^2 of endocrine area. We also calculated the area of synaptic structures/100 μm^2 of endocrine tissue. Mean area of mitochondria in obese and lean animals was calculated.

Data analysis

The area of TH + fibers, the number of TH + cells and NPY + cells were counted and results are given as means ± S.E.M. Differences between means were analyzed by *t*-test or ANOVA when different age groups were compared (InStat, GraphPad; San Diego, CA). For all analysis, $P < 0.05$ was used to declare statistical significance and P =NS was used to declare statistical not significant. If not otherwise stated, the results are given as mean ± S.E.M. of n =5 animals for each group.

Results

Body weight and metabolic parameters

The metabolic features of obese mice progressively worsened with age. Thus, body weight increased in both *ob*/*ob* and *db*/*db* mice in a stepwise fashion compared with haploinsufficient controls between 6 and 15 weeks of age (data not shown).

Fasted glucose levels increased significantly in 15-week-old *db*/*db* mice. Plasma glucose, insulin and HOMA in 15 weeks old HFD mice were similar to that of *ob*/*ob* mice. (Supplementary Fig. S1)

Islet morphometry

We measured endocrine pancreas size by assessing the proportion of pancreatic tissue occupied by islets; we also surveyed islet density and mean area.

Altogether, our morphometric data indicate that the increased endocrine parenchyma in obese mice (both 6-and 15-week-old) is mainly due to islet hypertrophy and that there is a tendency to decreased islet mass in *db*/*db* mice compared to *ob*/*ob* mice at 15 weeks (data not shown). This is in line with the demonstrated ability of *ob*/ *ob* mice to compensate, for insulin resistance, as demonstrated in previous works [22].

Immunohistochemistry with anti-insulin antibodies showed that most of the endocrine parenchyma was composed by insulin immunoreactive cells both in lean and obese animals at all ages. Insulin immunoreactivity was weaker in islets of 15-week-old *db*/*db* mice (Fig. 1).

Tyrosine hydroxylase and Neuropeptide Y immunohistochemistry

Given the inhibitory action of noradrenaline and NPY on pancreatic insulin secretion [23,24], we sought to address whether content of these neurotransmitters was altered in diabetic islets. To this end, we performed immunohistochemistry with antibodies anti-TH, a widely used marker of noradrenaline-containing cells and nerves [19] and anti-NPY.

TH + fibers were distributed throughout exocrine (peritubular, perivascular and interstitial locations) and endocrine parenchyma (Fig. 2A).

Quantification showed higher innervation of endocrine than exocrine parenchyma in all groups of animals. In 15-week-old *db*/*db* mice, islets showed an ~18-fold enrichment in innervation compared to exocrine pancreatic parenchyma, while in *ob*/*ob* mice they showed an ~11-fold enrichment (Fig. 2B).

Within the islet, we considered TH + fibers both at the periphery and in the center. The mean area of TH + fibers was significantly higher in 15-week-old obese *db*/*db* mice vs. their lean control and vs. 15-week-old *ob*/*ob* mice. We also observed a significant increase of TH + fibers in *db*/*db* 15-week-old vs. *db*/*db* 6-week-old mice (Fig. 2C).

In order to exclude the effect of leptin resistance in *db*/ *db* mice in the interpretation of the results, we also measured TH + fibers density in islets of HFD mice. Results showed a 1.5-fold increase of fibers in comparison with the chow diet group (data not shown).

Islets of lean and obese mice also contained TH + cells (Fig. 3A, B), whose nature is still unclear [25,26].

The density of TH + cells increased in islets of 15-week-old *db*/*db* vs. control mice, and was significantly greater than in *ob*/*ob* mice (Fig. 3C). Confocal microscopy analysis revealed cytoplasmic co-localization of TH+ and insulin in these cells (Fig. 3D).

We also measured NPY + cells both at the periphery (within the three peripheral rows of insular cells) and in the center of islets because NPY has inhibitory properties on pancreatic beta cells [18,27].

We found numerous NPY + cells within islets of both lean and obese mice and an increased density of NPY + cells in *db*/*db* mice. In contrast we found a decrease of NPY + cells in

ob/*ob* mice at 15 weeks compared to 6 weeks, but these differences was not significant (Fig. 4A).

The most striking difference between lean and obese mice was in the distribution of this cell type. In fact, quantitative analysis showed that they were present both at the periphery and in the center of islets in lean and in obese 6-week-old mice, whereas they were predominantly found in the central part of islets in 15-week-old mice, more evidently so in *db*/*db* mice (Fig. 4B, C).

Electron microscopy

Insulin-secreting beta cells are the predominant endocrine cell type in the rodent islet and show unique structural features that allow investigators to distinguish them from other endocrine cells. Shape, subcellular localization, and density of insulin granules are the salient features [28]. In obese animals of both ages, cells with electron microscopic features of beta cells showed hypertrophy of rough endoplasmic reticulum and Golgi complex, suggestive of increased insulin secretion, and consistent with the metabolic data of hyperinsulinemia. Beta cells of 15-week-old obese mice also showed hypertrophic mitochondria [29,30], with the mean area in both *ob*/*ob* and *db*/*db* mice higher than controls, in line with the increased function (Fig. 5C, I).

In addition, we detected beta cells that showed these characteristic features together with signs of degeneration in 15-week-old obese (mainly, *db*/*db*) mice (Fig. 5D–F). These degenerating cells were rare in islets of lean mice at any age.

Parenchymal non-myelinated nerve fibers were observed by electron microscopy within islets of both lean and obese mice. They were often filled with small empty synaptic-like vesicles; occasionally, we also observed dense core granules and small mitochondria. These fibers were in tight contact with parenchymal cells and near all had structural features of beta cells, consistent with the morphology of synaptoid contacts with beta cells (Fig. 5A, B). Quantitative analysis in 15-week-old mice showed that their density increased in obese mice, particularly in *db*/*db* mice (Fig. 5G, H). The increase was comparable to that found for TH + fibers.

Discussion

The progression from obesity to type 2 diabetes is often associated with beta cell failure [31–33] but the mechanism of this abnormality is unclear, arising as it does from a combination of functional and anatomic alterations in insulin secretion and beta cell number [11,13]. Metabolic data in the present study confirm earlier observations of increased beta cell mass in obese mice, associated with increased plasma insulin levels. But as compensation fails, islet mass gradually decreases and beta cells become depleted of their characteristic insulin secretory granules [11,13,22]. Accordingly, we observed a decrease in beta cell area and reduced insulin immunoreactivity in 15-week-old *db*/*db* mice that accompanied the onset of hyperglycemia. In contrast, *ob*/*ob* mice were able to maintain normal glucose levels at both ages examined, despite substantial insulin resistance, and this was associated with preserved islet mass and insulin immunoreactivity.

The decrease in islet mass is generally attributed to apoptosis, although we have recently provided evidence that beta cell dedifferentiation also plays a role in this process [34]. In this regard, it should be emphasized that, despite the longstanding observation that human and mouse islet show extensive adrenergic innervation [19,15], little is known about whether this feature undergoes changes during the progression of beta cell dysfunction in obesity related diabetes. To address this question, we studied islet innervation in *ob*/*ob* and *db*/*db* mice at two different stages in the development of their obesity and diabetes, corresponding to different compensatory stages in the natural history of beta cell dysfunction.

We focused on noradrenergic nerves and NPY + cells in light of the reported role of adrenergic agonists and NPY to inhibit insulin secretion [17,18,27].

Immunohistochemistry with anti-TH antibodies showed an age-dependent enrichment in fibers contacting endocrine cells in all groups of animals. Interestingly, TH + fiber area in diabetic islets from *db*/*db* mice was significantly larger than in non-diabetic *db*/+ controls as well as in obese non-diabetic *ob*/*ob* mice, consistent with the relationship between inhibition of insulin secretion and increased noradrenergic fiber content in diabetes [16,17].

Our findings are consistent with the notion of an inhibitory role of adrenergic innervations on insulin secretion, since it has been demonstrated that beta cells have more alpha2 adrenergic receptors (which inhibit insulin secretion) than alpha1 and beta2 (which enhance insulin secretion) [35]. Considering that leptin increase the sympathetic outflow [36], it is even more significant the observation that these mice (lacking leptin or its receptor) have an increased density of TH parenchymal fibers in their islets. Furthermore to exclude any leptin interference we measured TH fibers in islets of 15 weeks old HFD mice. We found a 1.5-fold increase in these mice that corresponded to that observed in *ob*/*ob* mice.

These findings prompted us to investigate the relationship between noradrenergic fibers and beta cells using electron microscopy.

This approach confirmed the presence of non-myelinated nerve fibers that made contact with parenchymal cells within islets of lean and obese mice, >90% of which had structural features of beta cells. This increased paralleled the increase in synaptic elements in direct contact with beta cells, and their increased density in obese mice, particularly *db*/*db*.

Islets of lean and obese mice also contained TH +cells whose nature is still unclear. Their frequency paralleled the increased frequency of cells with degenerative features in our electron microscopy studies. These degenerating cells were rare in islets of lean mice at any age. Confocal microscopy analysis revealed co-localization of TH+ and insulin in the cytoplasm of these cells, consistent with electron microscopy data showing insulin-like granules in degenerating cells and indicating that TH expression occurs during beta cells degeneration, as shown in previous studies [25,26]. It should be also considered that increased TH expression in beta cells and nervous fibers could affect autophagic mechanisms within the islet that are important for normal islet homeostasis [37].

We observed numerous NPY + cells within islets of both lean and obese mice. Density of NPY + cells increased in *db*/*db* mice, but the difference did not reach statistical significance. However, we did observe a striking difference in the distribution of these cells within islets of lean and obese mice. In the former, they localized both at the periphery and in the center of islets, whereas in the latter, especially at 15 weeks of age, they were predominantly found in the central part of the islets [38]. This change could be taken as indirect evidence of NPY-dedifferentiating beta cells or of cells with an inhibitory effect on insulin secretion/beta cell proliferation [34].

Overall, in this study, we have described an increased noradrenergic innervation of pancreatic islets, with increased TH + fibers making contact with beta cells in genetically obese mice. This is consistent with data from Myrsèn et al. showing that explanted beta cells are able to produce neurotrophic factors that could be responsible for increased noradrenergic innervation [39]. The increase of TH + fibers parallels a dramatic worsening of diabetes and a decrease of insulin secretion, especially in *db*/*db* mice. The observation of persistently elevated insulin in 15-week-old *db*/*db* mice could be explained by decreased insulin clearance, or by the capacity of residual pancreatic beta cells to compensate for insulin resistance, albeit temporarily. One limitation of our study is that we didn't assess the Disposition Index. But this lack of information is offset by extensive literature demonstrating insulin resistance in these models [22].

The onset of a mechanism that inhibits insulin secretion could be viewed as an additional mechanism of impaired beta cell function, worsened by concurrent insulin resistance.

We also show an increased number of NPY + cells in frankly diabetic *db*/*db* mice and a reduction in euglycemic *ob*/*ob* mice at 15 weeks. These data are in agreement with work fro Imai et al. who have observed that endogenous NPY tonically inhibits insulin secretion from islets and have reported a decrease in the levels of NPY mRNA in *ob*/ *ob* mice as a mechanism to increase insulin secretion when islets compensate for insulin resistance associated with obesity [40]. We are aware of the limitation of the approach used, which is especially based on morphology. This doesn't allow to draw definitive conclusions but it is a first important step mainly descriptive.

It remains to be determined whether these cells convey signals to inhibit insulin secretion, or whether they represent a consequence of beta cell hypertrophy/failure. We speculate that they inhibit insulin secretion in a paracrine manner, effectively preceding irreversible loss of beta cells.

In conclusion, our data raise the question of whether pharmacological inhibition of intra-islet noradrenergic transmission can play a role in the treatment of beta cell dysfunction in type 2 diabetes.

Supplementary Material

Refer to Web version on PubMed Central for supplementary material.

Acknowledgments

This work was supported by DIABAT Collaborative Project of the European Community's FP7, Grant agreement number HEALTH-F2-2011-278373 to SC.

References

1. Accili D, Ahrén B, Boitard C, Cerasi E, Henquin JC, Seino S. What ails the β-cells? Diabetes Obes Metab. 2010; 12(Suppl 2):1–3. [PubMed: 21029293]
2. Hotamisligil GS. Inflammation and metabolic disorders. Nature. 2006; 444:860–7. [PubMed: 17167474]
3. Bjorntorp P. Visceral obesity: a "civilization syndrome". Obes Res. 1993; 1:206–22. [PubMed: 16350574]
4. Bjorntorp P. Hormonal regulation of visceral adipose tissue. Growth Horm IGF Res. 1998; (Suppl 8):B:15–7.
5. Bjorntorp P. Visceral fat accumulation: the missing link between psychosocial factors and cardiovascular disease? J Intern Med. 1991; 230:195–201. [PubMed: 1895041]
6. Bruun JM, Lihn AS, Pedersen SB, Richelsen B. Monocyte chemo-attractant protein-1 release is higher in visceral than subcutaneous human adipose tissue (AT): implication of macrophages resident in the AT. J Clin Endocrinol Metab. 2005; 90:2282–9. [PubMed: 15671098]
7. Leahy JL. Pathogenesis of type 2 diabetes mellitus. Arch Med Res. 2005; 36:197–209. [PubMed: 15925010]
8. Cinti S, Mitchell G, Barbatelli G, Murano I, Ceresi E, Faloia E, et al. Adipocyte death defines macrophage localization and function in adipose tissue of obese mice and humans. J Lipid Res. 2005; 46:2347–55. [PubMed: 16150820]
9. Weisberg SP, Mc Cann D, Desai M, Rosenbaum M, Leibel RL, Ferrante AW Jr. Obesity is associated with macrophage accumulation in adipose tissue. J Clin Invest. 2003; 112:1796–808. [PubMed: 14679176]
10. Xu H, Barnes GT, Yang Q, Tan G, Yang D, Chou CJ, et al. Chronic inflammation in fat plays a crucial role in the development of obesity-related insulin resistance. J Clin Invest. 2003; 112:1821–30. [PubMed: 14679177]
11. Butler AE, Janson J, Bonner-Weir S, Ritzel R, Rizza RA, Butler PC. Beta-cell deficit and increased beta-cell apoptosis in humans with type 2 diabetes. Diabetes. 2003; 52:102–10. [PubMed: 12502499]
12. Jonas JC, Sharma A, Hasenkamp W, Ilkova H, Patanè G, Laybutt R, et al. Chronic hyperglycemia triggers loss of pancreatic beta cell differentiation in an animal model of diabetes. J Biol Chem. 1999; 14:4112–21.
13. De Fronzo RA. Lilly lecture 1988. The triumvirate: beta-cell, muscle, liver. A collusion responsible for NIDDM. Diabetes. 1987; 37:667–87.
14. Larsen CM, Faulenbach M, Vaag A, Vølund A, Ehses JA, Seifert B, et al. Interleukin-1-receptor antagonist in type 2 diabetes mellitus. N Engl J Med. 2007; 356:1517–2152. [PubMed: 17429083]
15. Chiu YC, Hua TE, Fu YY, Pasricha PJ, Tang SC. 3-D imaging and illustration of the perfusive mouse islet sympathetic innervation and its remodelling in injury. Diabetologia. 2012; 55:3252–61. [PubMed: 22930160]
16. Rodriguez-Diaz R, Speier S, Molano RD, Formoso A, Gans I, Abdulreda MH, et al. Noninvasive in vivo model demonstrating the effects of autonomic innervation on pancreatic islet function. Proc Natl Acad Sci U S A. 2012; 109:21456–61. [PubMed: 23236142]
17. Ahrén B. Autonomic regulation of islet hormone secretion-implications for health and disease. Diabetologia Rev. 2000; 43:393–410.
18. Ahrèn B, Ericson LE, Lundquist I, Lorèn I, Sundler F. Adrenergic innervation of pancreatic islets and modulation of insulin secretion by the sympatho-adrenal system. Cell Tissue Res. 1981; 216:15–30. [PubMed: 6112065]

19. Rodriguez-Diaz R, Abdulreda MH, Formoso AL, Gans I, Ricordi C, Berggren PO, et al. Innervation patterns of autonomic axons in the human endocrine pancreas. Cell Metab. 2011; 14:45–54. [PubMed: 21723503]
20. Borelli MI, Rubio M, Garcia ME, Flores LE, Gagliardino JJ. Tyrosine hydroxylase activity in the endocrine pancreas: changes induced by short-term dietary manipulation. BMC Endocr Disord. 2003; 3:2. [PubMed: 12659644]
21. Kiba T. Relationship between the autonomic nervous system and the pancreas including regulation of regeneration and apoptosis. Pancreas. 2004; 29:51–8.
22. Prentki M, Nolan CJ. Islet beta cell failure in type 2 diabetes. J Clin Invest. 2006; 116:1802–12. [PubMed: 16823478]
23. Bennet WM, Wang ZL, Jones PM, Wang RM, James RF, London NJ, et al. Presence of neuropeptide Y and its messenger ribonucleic acid in human islets: evidence for a possible paracrine role. J Clin Endocrinol Metab. 1996; 81:2117–20. [PubMed: 8964837]
24. Myrsén-Axcrona U, Karlsson S, Sundler F, Ahrén B. Dexamethasone induces neuropeptide Y (NPY) expression and impairs insulin release in the insulin-producing cell line RINm5F. Release of NPY and insulin through different pathways. J Biol Chem. 1997; 272:10790–6. [PubMed: 9099732]
25. Teitelman G, Alpert S, Hanahan D. Proliferation, senescence, and neoplastic progression of β cells in hyperplasic pancreatic islets. Cell. 1988; 52:97–105. [PubMed: 2894250]
26. Persson-Sjögren S, Forsgren S, Täljedal IB. Tyrosine hydroxylase in mouse pancreatic islet cells, in situ and after syngeneic transplantation to kidney. Histol Histopathol. 2002; 17:113–21. [PubMed: 11813861]
27. Ahrén B, Wierup N, Sundler F. Neuropeptides and the regulation of islet function. Diabetes. 2006; 55:98–107.
28. Lacy PE. Electron microscopy of the beta cell of the pancreas. Am J Med. 1961; 31:851–9. [PubMed: 14461448]
29. Jitrapakdee S, Wutthisathapornchai A, Wallace JC, MacDonald MJ. Regulation of insulin secretion: role of mitochondrial signalling. Diabetologia. 2010; 53:1019–32. [PubMed: 20225132]
30. Anello M, Lupi R, Spampinato D, Piro S, Masini M, Boggi U, et al. Functional and morphological alterations of mitochondria in pancreatic beta cells from type 2 diabetic patients. Diabetologia. 2005; 48:282–9. [PubMed: 15654602]
31. Campbell RK. Fate of the beta-cell in the pathophysiology of type 2 diabetes. J Am Pharm Assoc. 2009; 49(Suppl 1):S10–5.
32. Campbell RK, Neumiller JJ, White J, Sisson E, Kuhn C. Type 2 diabetes: epidemiology and treatment, pathophysiology, new therapeutics, and the evolving role of the pharmacist. J Am Pharm Assoc. 2009; 49(Suppl 1):S2.
33. Colagiuri S. Diabesity: therapeutic options. Diabetes Obes Metab. 2010; 12:463–73. [PubMed: 20518802]
34. Talchai C, Xuan S, Lin HV, Sussel L, Accili D. Pancreatic β cell dedifferentiation as a mechanism of diabetic β cell failure. Cell. 2012; 150:1223–34. [PubMed: 22980982]
35. Lacey RJ, Chan SL, Cable HC, James RF, Perrett CW, Scarpello JH, et al. Expression of alpha 2- and beta-adrenoceptor subtypes in human islets of Langerhans. J Endocrinol. 1996; 148(3):531–43. [PubMed: 8778232]
36. Collins S, Kuhn CM, Petro AE, Swick AG, Chrunyk BA, Surwit RS. Role of leptin in fat regulation. Nature. 1996; 380(6576):677. [PubMed: 8614460]
37. Ebato C, Uchida T, Arakawa M, Komatsu M, Ueno T, Komiya K, et al. Autophagy is important in islet homeostasis and compensatory increase of beta cell mass in response to high-fat diet. Cell Metab. 2008; 8(4):325–32. [PubMed: 18840363]
38. Fu M, Li X, Zhang M, Xian Y. Increased expression of neuropetide Y and its mRNA in STZ-diabetic rats. Chin Med J. 2002; 115:690–5. [PubMed: 12133536]
39. Myrsén U, Keymeulen B, Pipeleers DG, Sundler F. Beta cells are important for islet innervation: evidence from purified rat islet-cell grafts. Diabetologia. 1996; 39:54–9. [PubMed: 8720603]

40. Imai Y, Patel HR, Hawkins EJ, Doliba NM, Matschinsky FM. Insulin secretion is increased in pancreatic islets of neuropeptide Y deficient mice. Endocrinology. 2007; 148:5716–23. [PubMed: 17717054]

Appendix A. Supplementary data

Supplementary data related to this article can be found at http://dx.doi.org/10.1016/j.numecd.2013.09.006

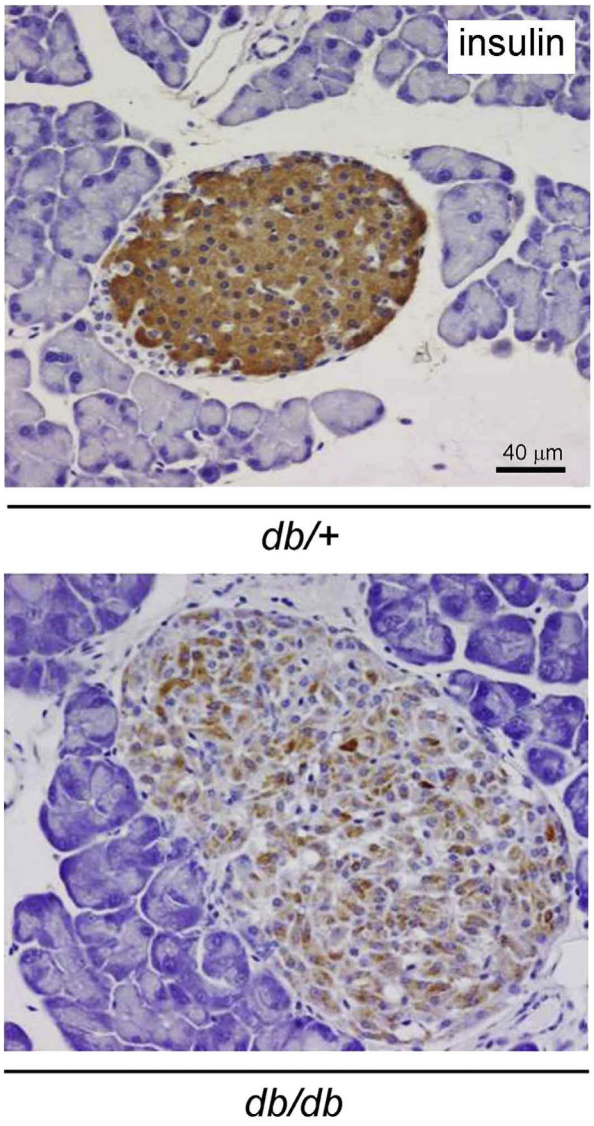

Figure 1.
Insulin IHC of 15 weeks old *db*/*db* mice shows weaker insulin immunoreactivity compared to control mice *db*/+.

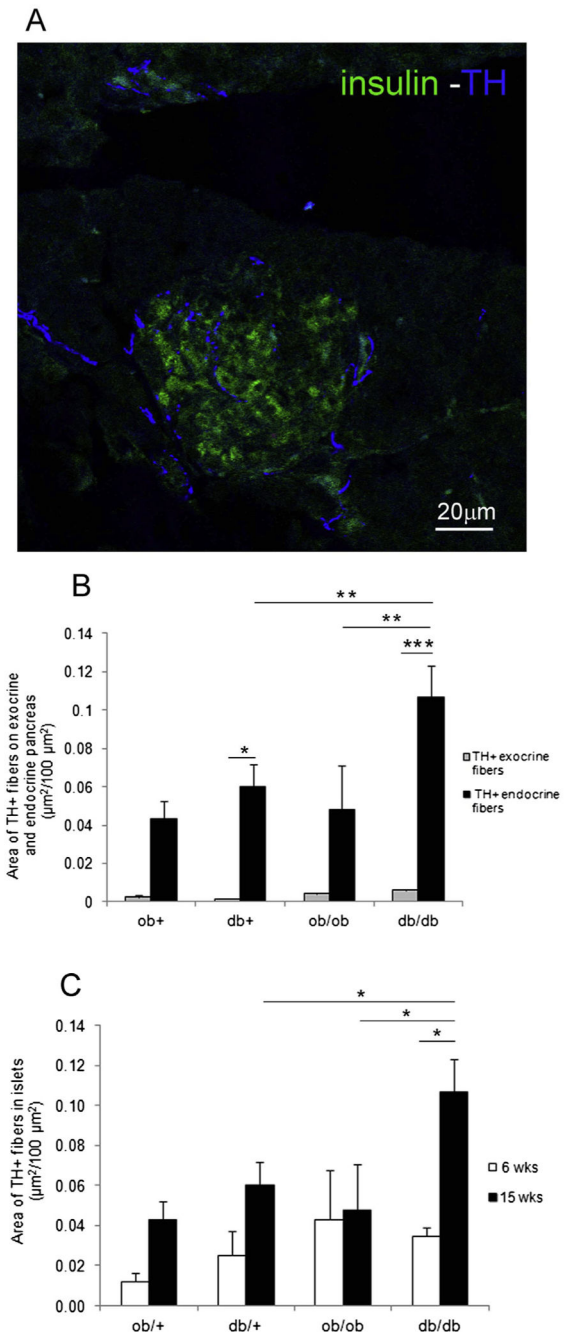

Figure 2.

TH positive fibers in islet of Langerhans. A) Confocal analysis of islet of Langerhans in *db*/*db* mouse. TH + fibers (blue) and insulin positive cells (green). B) Area of TH + fibers in endocrine and exocrine pancreas. C) Area of TH + fibers at 6 and 15 weeks. (**P* <0.05, ***P* <0.01, ****P* <0.001).

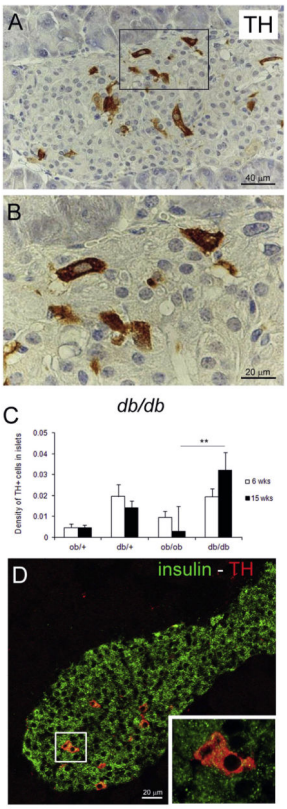

Figure 3.

TH positive cells in islet. A) IHC anti-TH in *db*/*db* mouse. B) Enlargement of squared area in A. C) Density of TH + cells at 6 and 15 weeks (**P <0.01). D) insulin (green) and TH (red) double staining. Enlargement of squared area shows co-localization of the two.

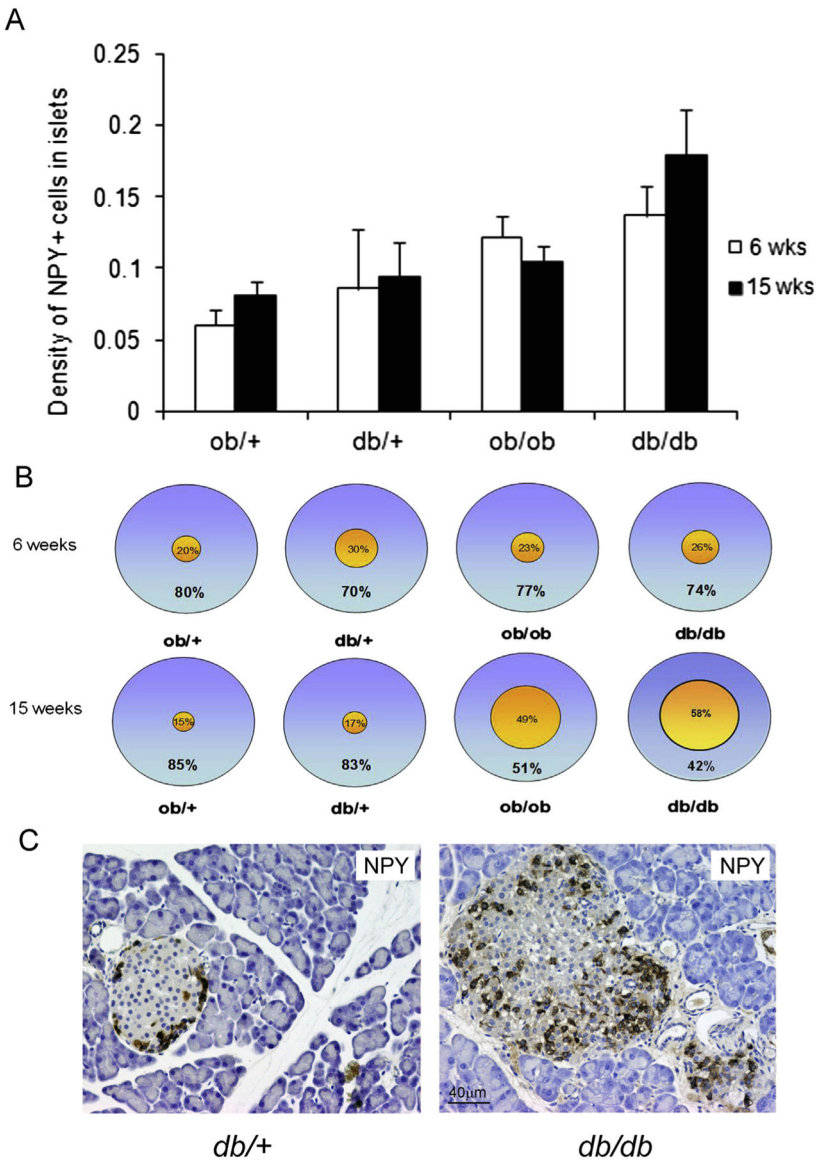

Figure 4.

A) Density at 6 and 15 weeks (*P* =*NS*). B) Percentage of peripheral and central distribution. The 15 weeks *db*/*db* mice have predominantly central distribution of NPY positive cells. At 15 weeks age old ***$P < 0.001$ of central positive cells in *db*/*db* vs. *db*/+; ***$P < 0.001$ of central positive cells *ob*/*ob* vs. *ob*/+; **$P < 0.01$ in *db*/*db* positive central cells *vs*. peripheral cells. C) Representative NPY + cells in *db*/*db* and *db*/+ 15-week-old mice.

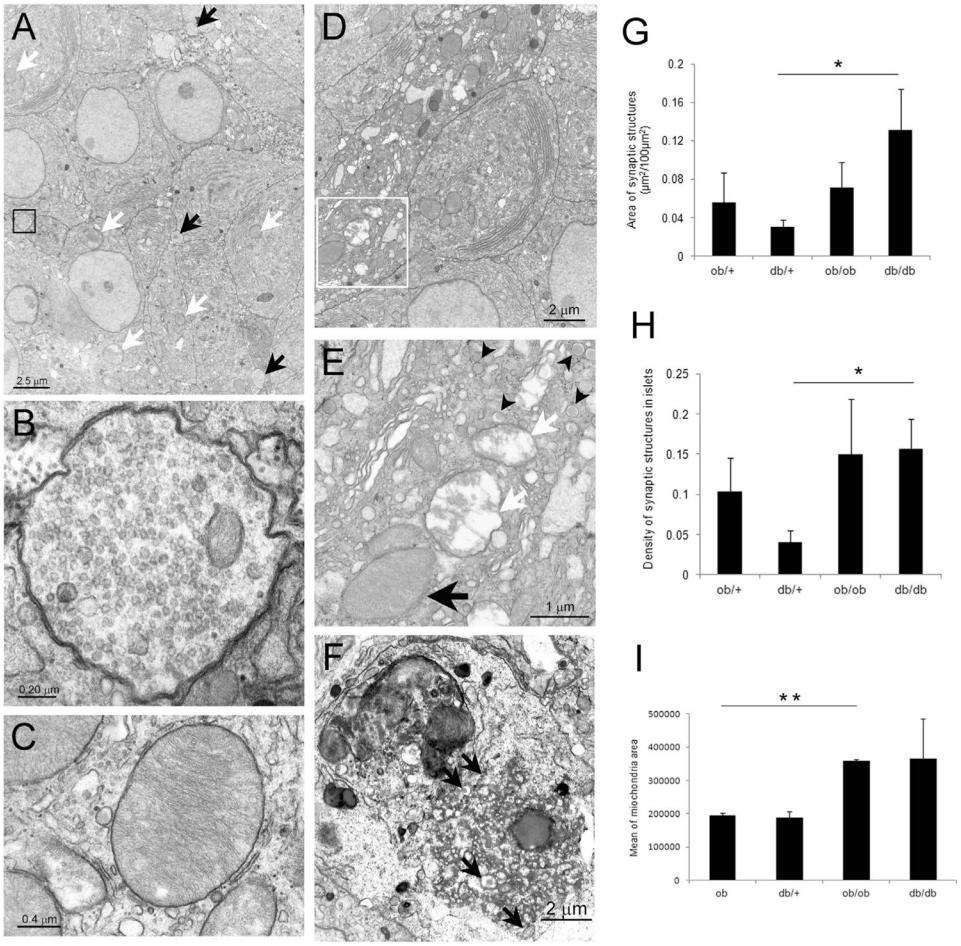

Figure 5.

Transmission electron microscopy of islet. A) TEM of islet in *db*/*db* mouse at 6 weeks; white arrows: large mitochondria (some indicated) of beta cells; black arrows: synaptoid structures. B) Enlargement of synaptoid structure shown in A (black square). C) Enlargement of representative large mitochondria of beta cells in *db*/*db* mouse. D) TEM of a cell with increased electron density in islet of 15 weeks old *db*/*db* mouse. E) Enlargement of squared area in D, showing typical granules (black arrowheads) and organelles with degenerative signs (white arrows: mitochondria with signs of degeneration); black arrow: large mitochondria. F) Lipofuscin laden lysosomes in the cytoplasm of an endocrine cell (see typical granules: black arrows) with signs of degeneration. G) Area of synaptic structures on islets at 15 weeks (**P* < 0.05). H) Density of synaptic structures at 15 weeks (**P* < 0.05). I) Mean area of mitochondria at 15 weeks (***P* < 0.01).